Proceedings of the 9th U.S. National and 10th Canadian Conference on Earthquake Engineering
Compte Rendu de la 9ième Conférence Nationale Américaine et
10ième Conférence Canadienne de Génie Parasismique
July 25-29, 2010, Toronto, Ontario, Canada • Paper No 1148

EFFECTIVE STIFFNESS OF HIGH-RISE CANTILEVER SHEAR WALLS

Ehsan Dezhdar[1] and Perry Adebar[2]

ABSTRACT

To determine the appropriate effective stiffness of concrete cantilever walls, the results from linear dynamic analyses using different effective stiffness assumptions for concrete walls were compared with the results from numerous nonlinear dynamic analyses. The nonlinear dynamic analyses were done using a nonlinear hysteretic model for concrete shear walls implemented into OpenSees. The study included 13 different walls with a range of nonlinear properties reflecting the range for typical concrete cantilever shear walls designed in Canada. The initial fundamental periods of the walls ranged from 0.5 to 4 seconds. Forty ground motions modified to fit a design spectrum were used. The elastic demand to flexural strength of walls (R) was varied from 0.5 to 5.0. It was found that the most important parameter is the ratio of elastic demand to strength of wall and that generally the effective stiffness of concrete walls does not reduce below about 50% of the stiffness of an uncracked wall for R values up to 5.0.

Introduction

One of the most important steps in the design of high-rise concrete shear wall buildings is estimating the maximum drift demands for the design earthquake, and in Canada, this is normally done using Response Spectrum Analysis (RSA). The effective stiffness (flexural rigidity) EI_e of the walls that are used in such analyses must account for the nonlinear response of walls due to cracking of concrete. Usually, a single reduction factor $\alpha = I_e/I_g$ is used for an entire concrete wall. Very different recommendations currently exist. FEMA 356 recommends a factor of 0.8 for uncracked walls and a factor of 0.5 cracked walls. The commentary to the 1995 New Zealand concrete code recommends a reduction factor of 0.25 for a concrete wall with no axial compression force and a factor of 0.35 for a wall with an axial compression force equal to $0.1f_c'A_g$. According to the Canadian concrete code for buildings (CSA A23.3 2004), the effective stiffness of concrete walls is a function of axial compression stress ratio $P/(f_c'A_g)$ and is equal to 0.7 for a wall with an axial compression force of $0.1f_c'A_g$.

In the current study, nonlinear dynamic analysis was used to estimate the effective stiffness of concrete cantilever shear walls. For this purpose, a simplified force – displacement relationship for concrete cantilever walls was developed. The model includes a backbone curve, rational rules for stiffness degradation, simplified rule for unloading, and an empirical rule for mid-cycle reloading. The results of the nonlinear dynamic analysis were used to estimate the stiffness reduction factor.

[1] Graduate Research Assistant, Dept. of Civil Engineering, University of British Columbia, Vancouver, V6T 1Z4
[2] Professor, Dept. of Civil Engineering, University of British Columbia, Vancouver, V6T 1Z4

Hysteretic Force – Displacement Relationship

Figure 1 shows a general schematic of the simplified force – displacement model. The model remains linear until shear force reaches V_{co}, which corresponds to shear at crack opening and is a function of lower – bound bending moment, M_{LB}, (Adebar and Ibrahim 2002) and lateral load distribution acting on the wall. Note that V_{co} is slightly smaller than the shear force at flexural cracking, V_{cr}. The slope of the linear segment, k_i, is the initial stiffness of the wall and depends on the wall height and gross section stiffness, EI_g. Once the shear force exceeds V_{co}, the loading path follows a nonlinear curve until it reaches the shear at the flexural capacity of the wall, V_n. A fourth – order polynomial defines the nonlinear section of the backbone curve. The solution of the polynomial requires five pieces of information to determine five constants of the polynomial. Four constants can be determined by inserting the position of start and endpoints of the curve as well as the slope of the curve at these points. The fifth constant can be obtained by defining an additional point that the curve must pass through between the start and endpoints of the curve.

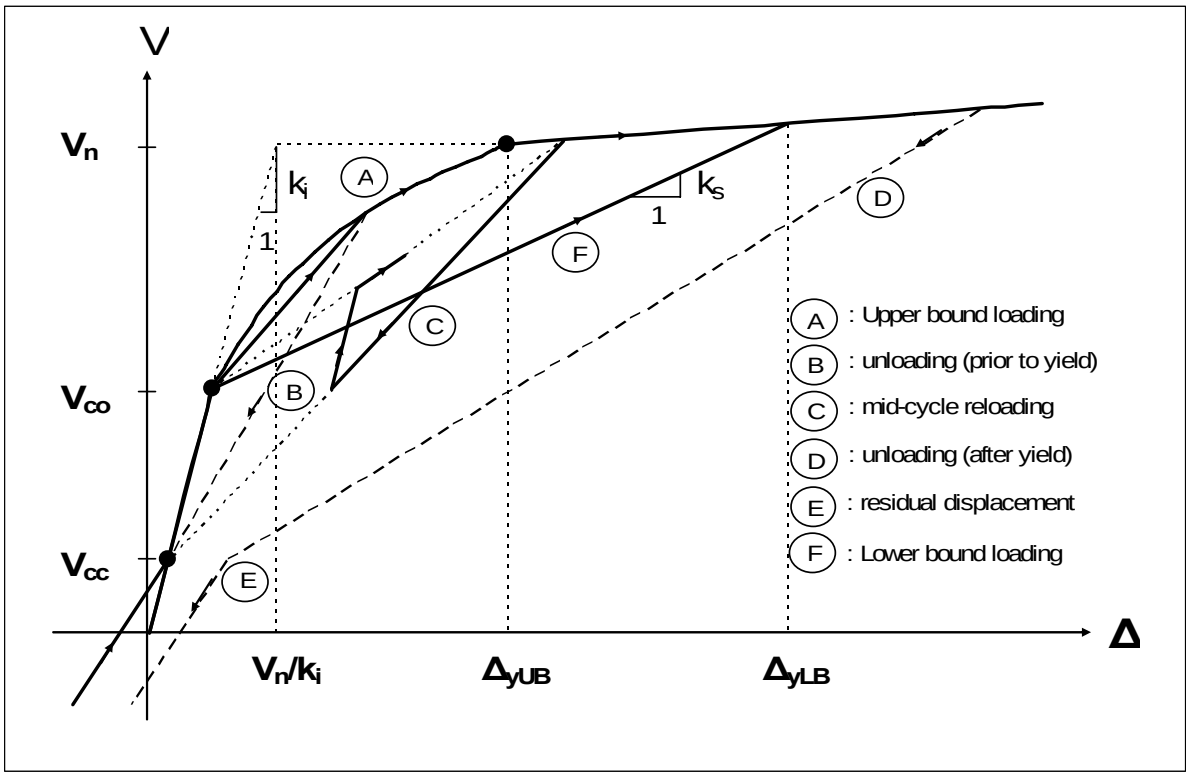

Figure 1. Hysteretic force – displacement response of cantilever shear walls used for nonlinear dynamic analysis.

The displacement at flexural capacity, Δ_{yUB}, is calculated by integrating the curvatures determined from the bending moment diagram using the trilinear moment- curvature relationship for the wall (Adebar and Ibrahim 2002). For displacements greater than Δ_{yUB}, the envelope is defined by a linear segment with a slope equal to 2% of the initial stiffness k_i to model strain hardening of the reinforcement.

The hysteretic path consists of a series of linear paths radiating from V_{co} to a point on the envelope corresponding to maximum previous displacement. The slope of the loading paths tend to decrease as displacement increases; however, in the cases that Δ_{yLB} is exceeded, all subsequent loading follows the lower bound trilinear reloading path regardless of maximum previous displacement. Lower bound yield displacement, Δ_{yLB}, is calculated by integrating curvatures determined from lower bound trilinear moment – curvature relationship over the height of the wall.

Unloading paths return linearly from maximum displacement to shear force at crack closing, V_{cc}. This parameter is a function of bending moment at which cracks will close due to the presence of axial load. For simplicity, it is assumed that the unloading point is located at the linear segment of the force – displacement envelope, i.e. zero residual displacement when pushing back the wall to the origin. Also shown in Fig.1 is the case that residual displacement is included by moving the unloading point from the linear segment of the backbone to a point with the same vertical coordinate but different horizontal coordinate values.

For mid-cycle reloading, the reloading path follows the initial slope k_i from the point where it leaves the unloading path. The reloading path intersects and follows a linear path from V_{co} to maximum previous displacement. In the cases that maximum previous displacement exceeds Δ_{yLB}, mid-cycle reloading follows the initial stiffness k_i until it joins the lower bound reloading path.

The hysteretic force – displacement model presented in Figure 1 can be fully determined by knowing key parameters k_i, V_{co}, V_n, Δ_{yUB}, Δ_{yLB}, and V_{cc}. The hysteretic model was implemented in OpenSees (Korchinski 2007) to conduct nonlinear dynamic analysis of concrete shear walls. The aim of this work is to investigate how the shape of force – displacement curve influences the effective stiffness. Therefore, it is necessary to generate a realistic range of the key parameters of the hysteretic model so that the walls included in the analysis can be regarded as a reasonable representation of practical shear walls.

The parameters of the hysteretic model are a function of the corresponding bending moment and the distribution of lateral loads over the height of the wall. Wall geometry, axial load level, and amount of vertical reinforcement can also influence the shape of the force – displacement curve. In order to develop a realistic range of the key parameters, a series of rectangular and flanged walls with different aspect ratios were studied. Web reinforcement ratio was assumed to be 0.25% for all walls. Flanged reinforcement ratio was varied from 0.5% to 2% for flanged walls and from 1% to 4% for rectangular walls. Axial load was also varied from 0 to $0.3f_c'A_g$. Table 1 presents the practical range of key parameters of the hysteretic force – displacement model. Each wall is labelled by a combination of “L” and “R” characters. “L” stands for Linear and the number after this character is a representative of the ratio of V_{co}/V_n. “R” stands for Reinforcement and is followed by a number which refers to the ratio of the secondary slope k_s to the initial slope k_i.

Table 1. Parameters that define the hysteretic response of the 13 walls considered in the study.

Walls	V_{co}/V_n	V_{cc}/V_n	k_s/k_i	$\Delta_{yUB}k_i/V_n$	$\Delta_{yLB}k_i/V_n$
W-L2-R3	0.20	-0.20	0.286	2.00	3.00
W-L2-R2	0.20	-0.20	0.167	2.70	5.00
W-L2-R1	0.20	-0.20	0.103	3.50	8.00
W-L4-R4	0.40	0.0	0.375	1.60	2.00
W-L4-R2	0.40	0.0	0.167	2.60	4.00
W-L4-R1	0.40	0.0	0.107	3.20	6.00
W-L5-R3	0.50	0.15	0.333	1.70	2.00
W-L5-R2	0.50	0.15	0.167	2.40	3.50
W-L5-R1	0.50	0.15	0.111	2.80	5.00
W-L6-R3	0.60	0.30	0.286	1.65	2.00
W-L6-R2	0.60	0.30	0.167	2.10	3.00
W-L6-R1	0.60	0.30	0.118	2.40	4.00
W-L8-R2	0.80	0.60	0.167	1.40	2.00

Ground Motions Used for Dynamic Analysis

Nonlinear dynamic analyses were performed using a set of forty ground motions taken from the suite of ground motions used in ATC 55 project (ATC 2005). Of these forty ground motions, twenty motions were recorded on site class B, and twenty motions were recorded on site class C. The ground motions correspond to eight different ground motions with magnitude M_s from 6.1 to 7.1 and peak ground acceleration from 48.9 to 504.2 cm/s^2. The forty ground motions were altered to a suite of modified ground motions such that the acceleration spectrum for these ground motions matches a prescribed target spectrum. The modified ground motions were created using computer program SYNTH (Naumoski 2001). This computer program modifies the initial recorded accelerogram (called initial or input accelerogram) until its spectrum matches the target spectrum. The target spectrum was a modified version of the National Building Code of Canada (NBCC 2005) design spectrum for Vancouver BC for soil type C. Figure 2 shows the NBCC design spectrum as well as the modified design spectrum. The actual NBCC design spectrum varies linearly between periods of 2 and 4 seconds and it remains constant for periods greater than 4 seconds, while the modified version of NBCC design spectrum decreases proportional to *1/T* for periods between 2 and 6 seconds. It should be mentioned that the spectral acceleration values at 2 and 4 seconds are identical for both spectrums. For modified design spectrum, the decrease was set proportional to $1/T^2$ for periods greater than 6 seconds. It means that spectral displacement ordinates remain constant over this period range.

Also shown in Figure 2 is the ASCE7-05 design spectrum for site class C for Seattle. The ASCE7-05 design spectrum consists of a linear segment where spectral acceleration increases with period, a flat plateau, a portion in which spectral acceleration decreases proportional to *1/T* for periods less than the long-period transition period, and finally a segment where the reduction in spectral values was set proportional to $1/T^2$. It can be observed that the modified version of the NBCC design spectrum is more consistent with ASCE7-05 design spectrum for longer periods. The modified NBCC design spectrum was used as the input design spectrum in computer

program SYNTH because the displacement spectrum corresponding to this design spectrum is more compatible with the mean displacement spectrum of the ground motions used in this analysis. The displacement spectrum for the forty modified ground motions is presented in Figure 3. The displacement spectrum corresponding to the modified design spectrum is also shown in Figure 3 with a thick line.

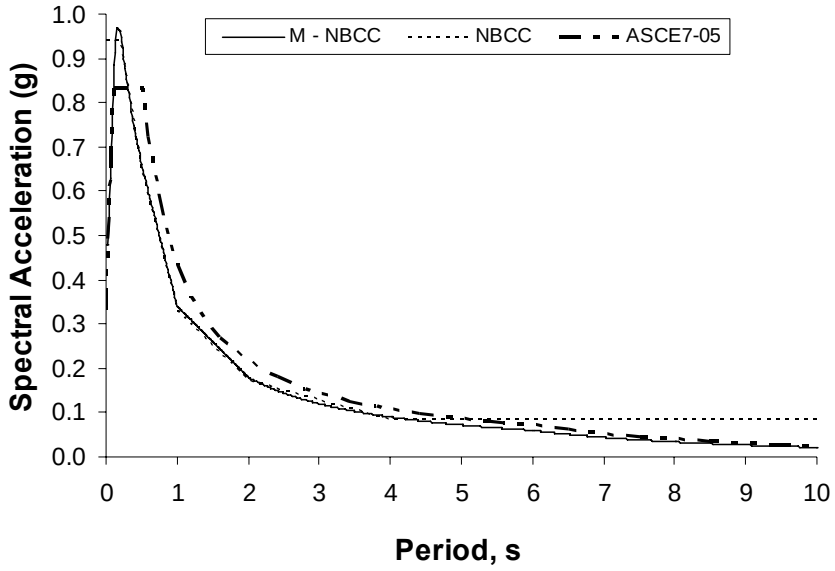

Figure 2. Comparison of Modified NBCC spectrum (M – NBCC) with NBCC design spectrum for Vancouver (NBCC) and ASCE7-05 design spectrum for Seattle (ASCE7-05).

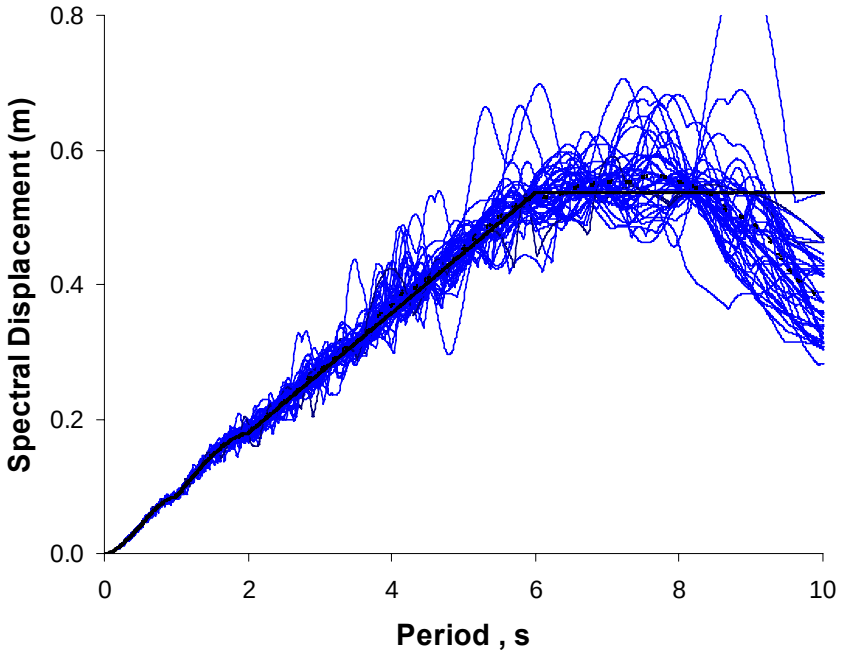

Figure 3. Displacement spectra for Modified ground motions.

Analysis Procedure

Modified ground motions were used as input ground motions in this study, and the damping was assumed to be 3 percent of critical damping. In addition, it was decided to scale ground motions to achieve different strength reduction factor *R*, rather than modifying the wall strength for various periods. It was done since all structural walls have the same initial stiffness and flexural capacity. It should be noted that strength reduction factor was defined as the ratio of the elastic force demand over the wall strength. Period of the structural walls was varied from 0.5 second to 4.0 seconds at 0.5 second intervals and for each period, a range of *R* values between 0.5 and 5.0 was considered. All structural walls were modelled as single degree of freedom systems. The walls have the force – displacement relationship similar to what was shown in Figure 1. All nonlinear time history analyses adopted the Newmark integration method with coefficients $\beta = 0.5$ and $\gamma = 0.25$. The time step was set equal to 0.005 s. The Newton-Raphson iteration method was used to satisfy equilibrium at each time step. The mass *m* of the SDOF system was adjusted in order to achieve different periods, and it was kept constant for each respective period. This approach required using different masses for different periods because the initial stiffness k_i was kept equal for all structural walls.

For each period and R value, maximum nonlinear displacement of the structural walls was recorded for the forty ground motions. The mean nonlinear displacement of the ground motions was then used to define the effective period and consequently effective stiffness. Effective period was defined as the period of an equivalent linear system with the same spectral ordinate as the mean displacement from nonlinear time history analysis. For the modified ground motions, however, the mean displacement spectrum for the forty ground motions matched the design spectrum very well (Figure 3). Therefore, using either design spectrum or mean of the ground motions would result in the same effective periods. However, the design spectrum was used for modified ground motions since it varies linearly for the periods ranging from 2 to 6 seconds, and therefore effective period can be determined by interpolating between the elastic displacements at the initial period and period of 6 seconds. The effective stiffness is determined from the effective period and the stiffness reduction factor α is determined from the ratio of stiffnesses, i.e. $\alpha = k_e/k_i$. The stiffness reduction factor is assumed to be the ratio of effective flexural rigidity EI_{eff} to gross flexural rigidity EI_g.

Analysis Results

The results of the analysis for three periods of 1.0, 2.0 and 3.5 seconds for the thirteen walls are shown in Figure 4 through 6. The results correspond to the mean nonlinear displacement of the forty modified ground motions at a specific *R* value and initial period. Note that it was also possible to determine effective stiffness reduction factors from the mean plus one standard deviation displacements. Although reduction factors from mean plus one standard deviation are less than those corresponding to mean nonlinear displacements, the difference is not significant since the forty ground motions are fitted to the design spectrum and hence the standard deviation for these ground motions are much less than the unmodified ground motions.

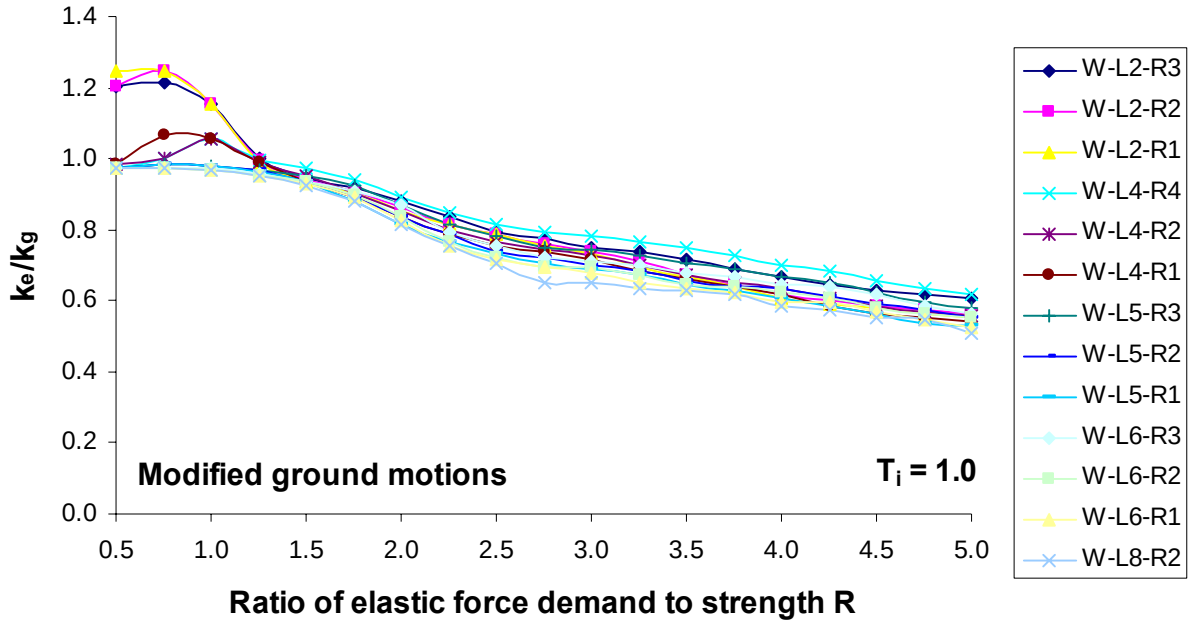

Figure 4. Stiffness reduction factors for thirteen different walls with an initial period of 1 s.

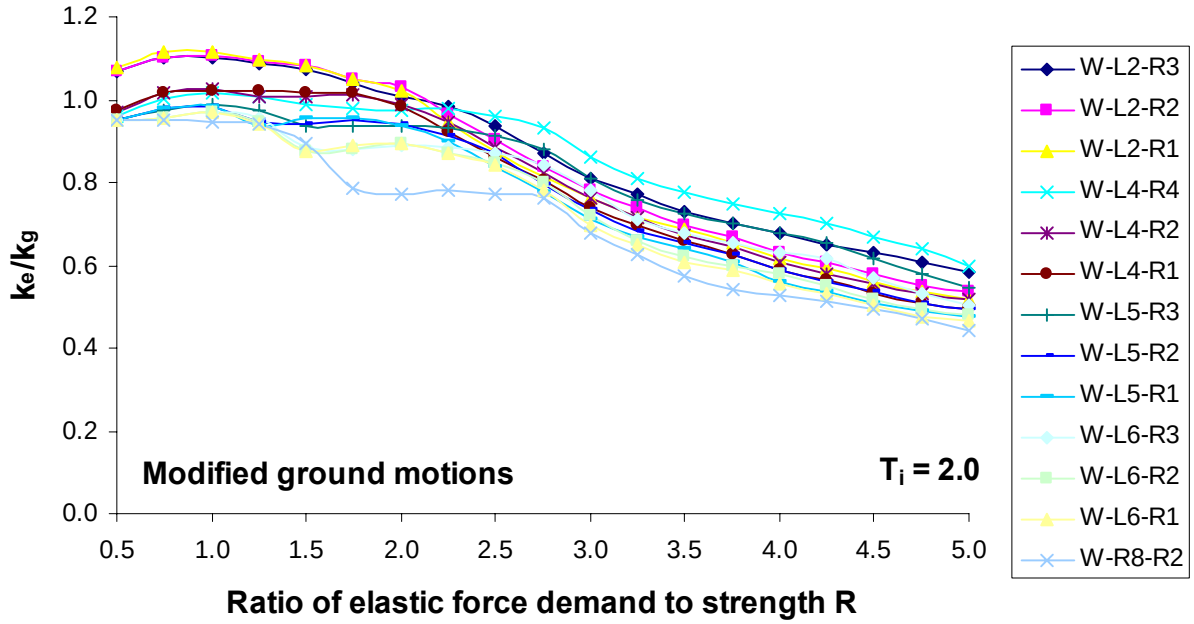

Figure 5. Stiffness reduction factors for thirteen different walls with an initial period of 2 s.

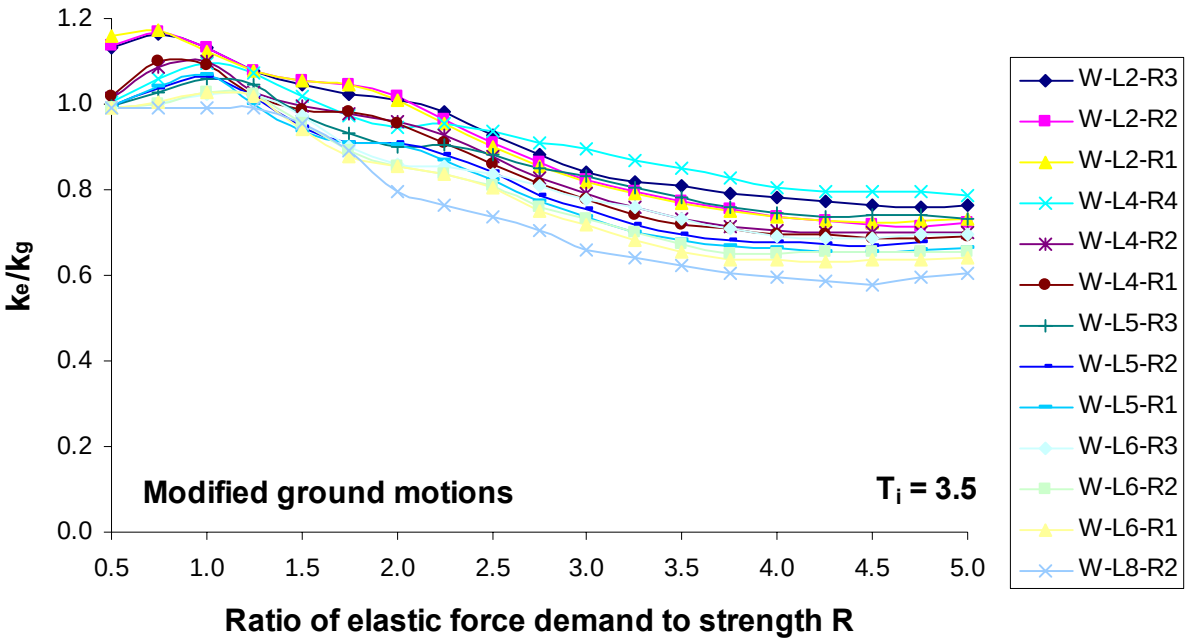

Figure 5. Stiffness reduction factors for thirteen different walls with an initial period of 3.5 s.

Several observations can be made regardless of which initial period was used in the analysis: (a) effective stiffness reduction factor is close to 1.0 for low R values. This means that effective period of the equivalent linear system is nearly the same as the initial period of the nonlinear model. It happens since most of the walls have barely passed the cracking point at low R values, and therefore most of the wall section is in the linear phase. As a result, nonlinear displacements are nearly equal to linear displacements, resulting in reduction factors close to 1.0. (b) thirteen walls described in Table 1 can be divided into groups of common V_{co}/V_n values. All walls in these groups have the same closing point, V_{cc}; however, these walls have different upper and lower bound force – displacement curves. The lowest effective stiffness within these groups belongs to the wall with the lowest lower bound stiffness. It happens since as the area between the loading and unloading decreases, hysteretic energy dissipation per cycle decreases and therefore, nonlinear displacement demand increases. Thus, walls W-L2-R3, W-L4-R1, W-L5-R1, and W-L6-R1 have lower effective stiffness reduction factors than other two walls with the same V_{co}/V_n values. (c) W-L8-R2 has consistently the lowest effective stiffness values regardless of the initial period. This wall has the smallest difference between loading and unloading paths meaning that the amount of energy dissipated by this wall is the least amongst the thirteen walls. This observation contradicts the initial prediction since W-L8-R2 has the highest axial load and consequently highest area under the curve. It means that if the area-under-the-curve method is used to determine effective stiffness, this wall must have the highest effective stiffness. However, the method to determine effective stiffness in this work is based on displacement demands and maximum displacement demands of a shear wall is influenced by both loading and unloading characteristics of force – displacement relationship.

Note that an additional analysis was carried out to examine the influence of energy dissipation on effective stiffness reduction factor. This was done by comparing the results of two walls having the same cracking point, upper and lower bound yield displacements but different

closing points. For this purpose, the crack closing point for wall W-L5-R3 was changed from $0.15V_n$ to $0.3V_n$. The initial period for both walls was assumed to be 2 seconds. The results of the analysis indicate that for wall W-L5-R3 effective stiffness reduction factor reduces from 0.99 at R = 1.0 to 0.54 at R = 5.0, while it drops from 0.95 to 0.49 for the same R values. This is equivalent to about 10% reduction for the highest R factor. This demonstrates that walls with lower energy dissipation generally tend to have higher displacement demand during earthquakes.

Figure 6 shows a summary of the effective stiffness reduction factor for all initial periods. An α value corresponding to a given period and R factor represents the mean of the α values for the thirteen walls. This figure indicates that at R = 1.0, α is equal to 1.0 regardless of the initial period, and as R increases, α drops to as low as 0.5 for 0.5 second initial period.

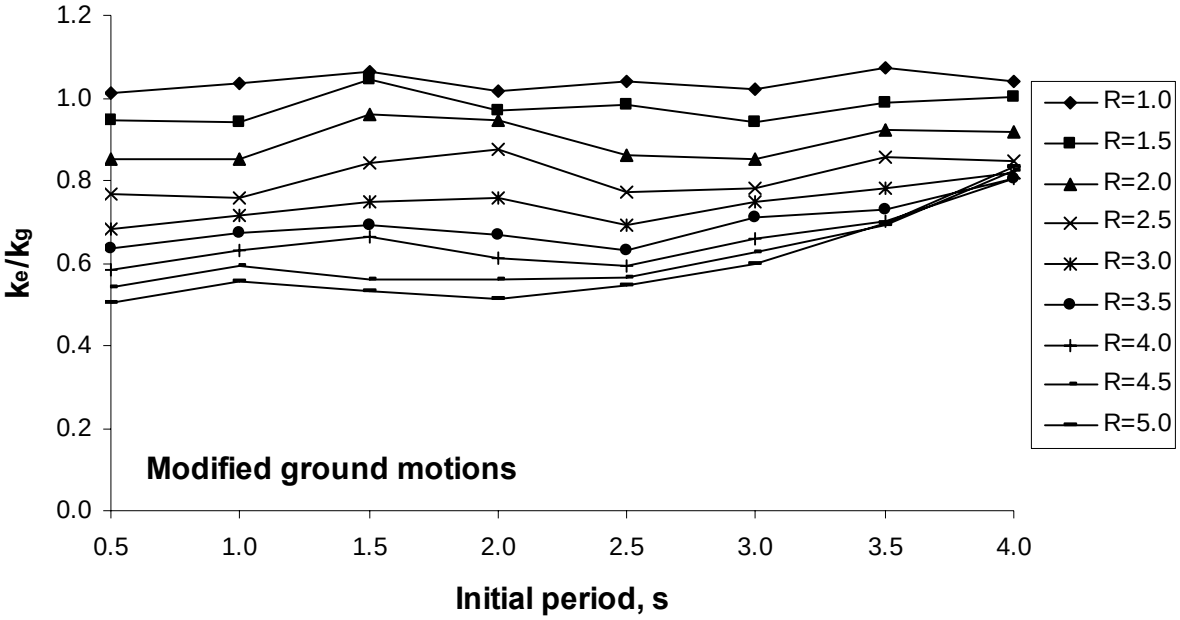

Figure 6. Summary of stiffness reduction factors for different initial periods and ratios of elastic force demand to strength R.

Summary and Conclusions

The aim of this work is to determine appropriate effective stiffness values for cantilever concrete shear walls in a way that the maximum drift demands using Response Spectrum Analysis (RSA) are good estimates of the displacement demands from nonlinear time history analysis. For this purpose, a specially developed nonlinear hysteretic model for concrete shear walls was implemented into OpenSees. The nonlinear model, including all rules for stiffness degradation, unloading, and mid-cycle reloading, were calibrated to the results of a recently completed large-scale test of a slender concrete shear wall. The study included 13 different walls with a range of nonlinear properties reflecting the range for typical concrete shear walls designed in Canada. The initial fundamental periods of the walls ranged from 0.5 to 4 seconds. Forty modified ground motions were used in the analysis and the range of elastic demand to strength of flexural strength of the walls (R) ranged from 1.0 to 5.0. The results of the study indicates that the most important parameter is the ratio of elastic demand to strength of wall, and that generally

the effective stiffness of concrete walls do not reduce below about 50% of the stiffness of an uncracked wall for *R* values up to 5.0. The axial compression stress ratio was found to have much less influence on the effective stiffness of concrete walls than previously thought. Opposite to what was expected, the wall with the highest axial compression stress ratio was found to actually have the lowest effective stiffness because that wall had proportionally less vertical reinforcement and thus less hysteretic damping. The conclusions from this study mean that significant changes are needed to the current Canadian concrete code provisions on effective stiffness of concrete shear walls given in Clause 21.2.5.

References

Adebar, P., and Ibrahim, A. M. M., "Simple Nonlinear Flexural Stiffness Model for Concrete Shear Walls," *Earthquake Spectra*, EERI, V. 18, No. 3, Aug. 2002, pp. 407-426.

ASCE7-05, 2005. "Minimum Design Loads for Buildings and Other Structures," ASCE/SEI 424 pp.

ATC, 2005, *Improvement of Nonlinear Static Seismic Analysis Procedure*, prepared by the Applied Technology Council for the Federal Emergency Management Agency, Redwood City. California.

CSA Committee A23.3 "Design of Concrete Structures: Structures (Design) – A National Standard of Canada" Canadian Standards Association 2004, Rexdale, Canada, 214 pp.

FEMA, 2000, *Prestandard and Commentary for the Seismic Rehabilitation of Buildings*, FEMA 356 Report, prepared by the American Society of Civil Engineers for the Federal Emergency Management Agency, Washington, D. C.

Korchinski, A. D. 2007. Investigation of Effective Stiffness of High-rise Concrete Shear Walls, *M.A.Sc. Thesis*, University of British Columbia, Vancouver.

National Research Council Canada (NRCC). 2005. National Building Code of Canada. Canadian Commission on Building and Fire Codes, National Research Council of Canada, Ottawa, Ontario.

Naumoski, N. D., 2001. Program SYNTH Generation of Artificial Accelerograms Compatible with a Target Spectrum, *Computer Program and Supporting Documentation*, Carleton University, Ottawa.

NZS 3101:Part 2, "Concrete Structures Standard Part 2-Commentary on the Design of Concrete Structures," Standards New Zealand, 1995.

Pacific Earthquake Engineering Research Center, "OpenSees – Open System for Earthquake Engineering Simulation," University of California, Berkeley, Calif.